BIOCHEMISTRY
including biophysical chemistry & molecular biology

Article

pubs.acs.org/biochemistry

The Photochemistry in Photosystem II at 5 K Is Different in Visible and Far-Red Light

Fredrik Mokvist, Johannes Sjöholm, Fikret Mamedov, and Stenbjörn Styring*

Molecular Biomimetics, Department of Chemistry-Ångström, Uppsala University, Ångström Laboratory, P.O. Box 523, S-751 20 Uppsala, Sweden

Supporting Information

ABSTRACT: We have earlier shown that all electron transfer reactions in Photosystem II are operational up to 800 nm at room temperature [Thapper, A., et al. (2009) *Plant Cell 21*, 2391−2401]. This led us to suggest an alternative charge separation pathway for far-red excitation. Here we extend these studies to a very low temperature (5 K). Illumination of Photosystem II (PS II) with visible light at 5 K is known to result in oxidation of almost similar amounts of Y_Z and the Cyt b_{559}/Chl_Z/Car_{D2} pathway. This is reproduced here using laser flashes at 532 nm, and we find the partition ratio between the two pathways to be 1:0.8 at 5 K [the partition ratio is here defined as (yield of Y_Z/$CaMn_4$ oxidation):(yield of Cyt b_{559}/Chl_Z/Car_{D2} oxidation)]. The result using far-red laser flashes is very different. We find partition ratios of 1.8 at 730 nm, 2.7 at 740 nm, and >2.7 at 750 nm. No photochemistry involving these pathways is observed above 750 nm at this temperature. Thus, far-red illumination preferentially oxidizes Y_Z, while the Cyt b_{559}/Chl_Z/Car_{D2} pathway is hardly touched. We propose that the difference in the partition ratio between visible and far-red light at 5 K reflects the formation of a different first stable charge pair. In visible light, the first stable charge pair is considered to be $P_{D1}{}^+Q_A{}^-$. In contrast, we propose that the electron hole is residing on the Chl_{D1} molecule after illumination by far-red light at 5 K, resulting in the first stable charge pair being $Chl_{D1}{}^+Q_A{}^-$. Chl_{D1} is much closer to Y_Z (11.3 Å) than to any component in the Cyt b_{559}/Chl_Z/Car_{D2} pathway (shortest Chl_{D1}−Car_{D2} distance of 28.8 Å). This would then explain that far-red illumination preferentially drives efficient electron transfer from Y_Z. We also discuss mechanisms for accounting for the absorption of the far-red light and the existence of hitherto unobserved charge transfer states. The involvement of two or more of the porphyrin molecules in the core of the Photosystem II reaction center is proposed.

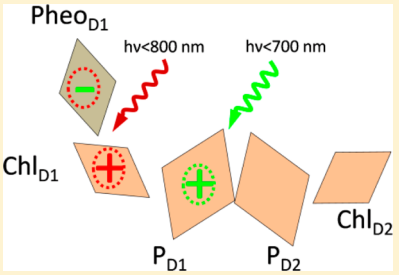

The quantum yield of oxygenic photosynthesis is known to decrease dramatically at wavelengths above 700 nm.[1] This phenomenon, known as the red drop from the classical experiments by Emerson[2,3] and Duysens,[4] led to the establishment of the concept of two separate photosystems, Photosystem I and Photosystem II, working cooperatively to drive the long-range electron transfer in the thylakoid membranes of plants and algae. The spectral properties of the isolated photosystems are often defined with respect to the primary chlorophyll electron donors, P_{680} in PS II and P_{700} in PS I. The molecular identity of the primary donor and the primary charge separation reactions that occur after photoexcitation of the reaction centers are much studied. In particular, this holds for PS II where the oxidative chemistry conducted by the components on the donor side puts formidable chemical and physical demands on the participating components.

A Chl component denoted P_{680} has long been known to be the primary electron donor in PS II.[5−9] The subscript indicates that the absorption maximum of the Q_y band is around 680 nm for the primary electron donor in PS II. Despite this, oxygen evolution can be induced by >700 nm light in green algae,[10] and in sunflower leaves, oxygen evolution was observed using wavelengths of ≤780 nm.[11] Charge separation in PS II has also been observed with 730 nm light at ultralow temperatures.[12−14] Recently, we took the studies of the far-red photochemistry further in a detailed spectroscopic investigation of most of the individual electron transfer reactions in PS II, including turnover of the $CaMn_4$ cluster, oxidation of Y_Z, reduction of $Pheophytin_{D1}$ ($Pheo_{D1}$), Q_A, and Q_B, etc. (see below). All these individual steps were observed after single flashes of ≤780 nm light at room temperature. In photoaccumulation experiments using far-red light, the PS II photochemistry was detectable up to 800 nm.[15] These findings led us to suggest an alternative charge separation pathway for far-red excitation. In this mechanism, a low-energy state denoted X* is formed in PS II after far-red light excitation. X* then triggers the charge separation and reduces pheophytin and oxidizes Y_Z but is working with an energetic margin lower than that of normal P_{680}*. We also proposed that X* was the excited state from a known chromophore in PS II that however had not previously been observed and linked to PS II primary photochemistry.[15]

Photosystem II (PS II) is a multisubunit protein complex in the thylakoid membranes of plants, cyanobacteria, and green algae that performs light-driven water oxidation and concomitant plastoquinone reduction. The light-driven electron transfer is conducted by a chain of redox components, all bound to the heterodimer of proteins D_1 and D_2 (Scheme 1).

Received: November 3, 2013
Revised: June 11, 2014
Published: June 11, 2014

dx.doi.org/10.1021/bi5006392 | *Biochemistry* 2014, 53, 4228−4238

Another important redox component in the PS II reaction center is Cyt b_{559}, which contains a heme group bound to the two membrane-spanning subunits psbE and psbF.[16]

Scheme 1

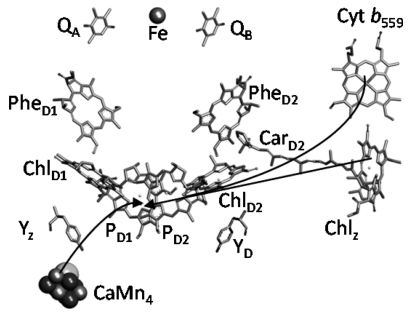

After the absorption of a photon by antenna subunits in PS II, subsequent excitation energy transfer occurs to the reaction center Chls constituting primary donor P_{680}. P_{680} is composed of four Chl molecules in the D_1/D_2 heterodimer denoted Chl_{D1}, Chl_{D2}, P_{D1}, and P_{D2} (Scheme 1[16]). The excitation of P_{680} triggers the initial charge separation between P_{680} and the primary electron acceptor pheophytin, giving rise to the $P_{680}^+Pheo^-$ primary radical pair. The exact path for the first step(s) in the primary charge separation has been much discussed. This originates from the fact that the four Chl pigments constituting P_{680} and the two pheophytins are all rather weakly electronically coupled to each other. The couplings are weak if compared to the two strongly coupled bacteriochlorophylls in the special pair in purple bacteria.[7,8,17−19] Thus, in the reaction center of PS II, there are six pigments that are all weakly coupled. This complicates the analysis of the events after a light excitation in PS II because the excitation energy can be localized on any of six pigment molecules. The result is that the primary charge separation might develop along different paths. Consequently, several different charge pairs like $P_{D1}^+P_{D2}^-$, $P_{D1}^+Chl_{D1}^-$, $Chl_{D1}^+Pheo_{D1}^-$, etc., might occur during the primary reaction.[6,8] Shortly after these first events, the $P_{D1}^+Pheo_{D1}^-$ charge pair dominates and P_{D1}^+ is often synonymous with P_{680}^+.[8,21] In a recent study in the D1/D2 reaction center preparation (lacking most PS II subunits, the $CaMn_4$ complex, Q_A, Q_B, and functional Y_Z) that was conducted at 77 K, evidence of two charge separation pathways was provided.[20] In one fraction of the centers, the first charge pair was $Chl_{D1}^+Pheo_{D1}^-$, and in another fraction of the centers, it was $P_{D1}^+Chl_{D1}^-$. In both cases, the system evolved to the final $P_{D1}^+Pheo_{D1}^-$ charge pair via charge equilibration reactions among the pigments. It was suggested that similar reactions also might occur in more intact PS II, although they are difficult to study there because of the many Chl molecules present in all such preparations.

Regardless of which exact primary charge separation event occurs, the electron finally arrives at $Pheo_{D1}$, creating the $Pheo_{D1}^-$ radical. From $Pheo_{D1}^-$, the electron is then transferred to the primary (Q_A) and secondary quinone acceptors (Q_B).[1,9] After two charge separation events, Q_B has been reduced two times and leaves the Q_B site on the D_1 protein in the quinol form (Q_BH_2). It is then replaced by an oxidized quinone from the quinone pool in the thylakoid membrane.

The situation on the electron donor side of PS II is more complex and involves many redox components that conduct a multitude of electron transfer and proton-coupled electron transfer reactions (Scheme 1). P_{680}^+ (P_{D1}^+)[21] is normally reduced rapidly (within nanoseconds) by the nearby redox active tyrosine residue (Y_Z) on the D_1 protein forming the $Y_Z^\bullet$ radical. In this context, it is relevant that P_{D1} is closest to Y_Z of the chlorophylls in the reaction center. $Y_Z^\bullet$ is in turn reduced from the $CaMn_4$ cluster, which is the catalytic site of water oxidation (Scheme 1).[22] In this report, we denote this the Y_Z/$CaMn_4$ pathway. After four charge separation events, the $CaMn_4$ cluster has accumulated four oxidation equivalents leading to the oxidation of water and evolution of molecular oxygen. During catalysis, the $CaMn_4$ cluster cycles in a stepwise manner through five intermediate redox states called S_n states (n = 0−4).[22,23] Oxidation of the S_3 state leads to the formation of the transient S_4 state, which drives the final formation of oxygen, and the $CaMn_4$ cluster returns to the S_0 state, which is the most reduced state. The S_1 state is the dominating state in the dark, while the S_2 and S_3 states are metastable intermediates that decay back to the S_1 state on a time scale of seconds to minutes. The S_0 state is slowly converted to the S_1 state during a long dark incubation.[24]

At physiological temperatures, P_{680}^+ reduction is completely dominated by electrons arriving from the $Y_Z/CaMn_4$ pathway leading to efficient water oxidation. To accomplish Y_Z oxidation that occurs at ∼1.2 V[25] and eventually water oxidation, the oxidizing power of P_{680}^+ is ∼1.4 V,[8,26] which is one of the most oxidizing potentials that occur in an enzymatic reaction. Therefore, in cases in which Y_Z is for some reason unable to deliver an electron quickly, P_{680}^+ can also be reduced by auxiliary electron transfer pathways from other redox active species in the vicinity. The most important is the so-called Cyt $b_{559}/Chl_Z/Car_{D2}$ pathway where Chl_Z and Car_{D2} are both bound to the D_2 protein. Here Cyt b_{559} or Chl_Z provides an electron to P_{680}^+ via Car_{D2}. The donation of an electron to P_{680}^+ from a chlorophyll molecule and Cyt b_{559} was first observed by optical spectroscopy at low temperatures in PS II lacking the $CaMn_4$ cluster[27,28] and has since been extensively studied.[29−38]

This alternative pathway becomes active and plays an important role in PS II under conditions where the Y_Z/$CaMn_4$ pathway is inhibited or functions less well. Such conditions occur, for example, at low temperatures (studied here), after photoinhibition or following different treatments that remove or inactivate the $CaMn_4$ cluster.[32−34] In early work, EPR spectroscopic analysis of S_2-state multiline signal formation and Cyt b_{559} oxidation was applied to study the competition between the $Y_Z/CaMn_4$ pathway and the Cyt $b_{559}/Chl_Z/Car_{D2}$ pathway in intact PS II between 77 K and room temperature.[29] More recently, the competition between the two pathways has also been investigated at 5−10 K.[39−41] At these temperatures, the $CaMn_4$ cluster is unable to turn over but Y_Z can still provide an electron in 40−50% of the PS II centers depending on the S state while the Cyt $b_{559}/Chl_Z/Car_{D2}$ pathway reduces the remaining part of P_{680}^+.

Our earlier study of electron transfer triggered by the absorption of far-red light was performed at room temperature where the reactions leading to the oxidation of water all were functional to ∼800 nm.[15] However, although charge separation has been observed after far-red illumination up to 730 nm,[13] the function of the different electron donor pathways has not been studied as a function of wavelength at low temperatures, where most thermally activated processes will be limited.

dx.doi.org/10.1021/bi5006392 | Biochemistry 2014, 53, 4228−4238

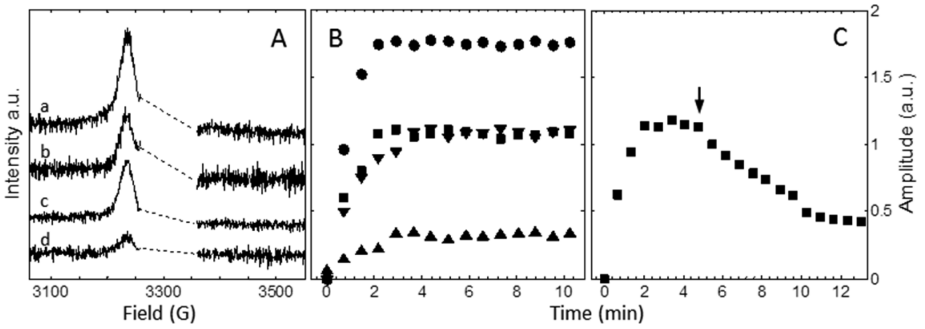

Figure 1. Wavelength-dependent induction of the split S_1 EPR signal at 5 K in PS II. (A) Induction of the split S_1 EPR signal achieved by flash illumination of PS II-enriched membranes at 5 K for 10 min. The EPR spectra represent flashing at 532 nm (spectrum a), 730 nm (spectrum b), 740 nm (spectrum c), and 750 nm (spectrum d). The $g = 2$ region containing the large spectrum from $Y_D^\bullet$ was removed for the sake of clarity. (B) Induction of the split S_1 signal reflecting $Y_Z^\bullet$ formation. The signal was induced at 5 K by laser flashes provided at 532 (●), 730 (■), 740 (▼), or 750 nm (▲). The flashing (5 Hz) was started at $t = 0$ and continued for 10 min in total. An EPR spectrum was recorded during the flashing at the indicated time points. Each point represents the amplitude of the split S_1 signal at $g = 2.035$. (C) Formation and decay of the split S_1 EPR signal induced by flash illumination at 730 nm followed by decay in the dark. The laser flash illumination was turned off after 5 min, indicated with an arrow. EPR conditions: microwave frequency, 9.28 GHz; microwave power, 25 mW; modulation amplitude, 10 G; temperature, 5 K.

In this study, we use EPR spectroscopy to quantify the far-red-induced electron donor reactions that take place in PS II at 5 K. We show that the discrimination between the two electron donor pathways is different after illumination with green (visible) or far-red light. Our results have important implications both for the charge separation mechanism and for the molecular identity of the pigment(s) constituting primary donor P_{680}^+ after far-red illumination.

MATERIALS AND METHODS

Growth Conditions. Spinach (*Spinacia oleracia*) was grown hydroponically as described previously[42] at 20 °C under cool white fluorescent light (dysprosium lamp, Osram Power star HQI-E 400W/DV, 300 μE m^{-2} s^{-1}), with light−dark periods of 12 h.

PS II Membrane Preparation. Two different oxygen-evolving PS II membrane preparations from spinach were used in this study. The first preparation was obtained according to ref 43 with the soft 20 min detergent treatment and the second preparation, BBY type,[44] with the standard 30 min detergent treatment after an additional membrane stacking step.[45,46] Preparations were resuspended in a buffer containing 25 mM MES (pH 6.1), 400 mM sucrose, 15 mM NaCl, and 3 mM $MgCl_2$ for storage at −80 °C, at a Chl concentration of 6−10 mg/mL. It should also be mentioned that both our preparations show no detectable room-temperature $Y_Z^\bullet$ signal indicative of the damaged PS II centers.

Synchronization of the OEC to the S_1 State. For the experiments in which PS II was to be exposed to flashes at 5 K, the samples were diluted to a final concentration of 2 mg of Chl/mL and preflashed at 20 °C according to ref 47 to achieve a fully homogeneous sample synchronized in the S_1 state and the acceptor side with the reduced (Fe^{2+}) non-heme iron.

Quantification of Photosystem I. Photosystem I was quantified in the PS II-enriched membranes by oxidation with 10 mM ferricyanide $K_3[Fe(CN)_6]$ for 5 min at 20 °C. The resulting EPR spectrum of P_{700}^+ was obtained by subtraction of the large EPR signal from $Y_D^\bullet$, recorded in the same sample before chemical oxidation.[42] The amount of P_{700}^+ radical was quantified by comparison to the fully oxidized $Y_D^\bullet$ radical ($Y_D^\bullet$ has one radical per PS II center), which was used as an internal standard.[42]

Laser Illumination. Flashes were provided by a Spectra Physics PRO-290 Q-switched Nd:YAG laser (6 ns flashes) equipped with a Spectra Physics Quanta Ray MOPO 730 optical paramagnetic oscillator to achieve the desired wavelengths (bandwidth of flash of ±0.1 nm). To avoid any possible leak-through of unwanted visible light, the laser beam was passed through a RG9 cutoff filter when far-red wavelengths were used. To study electron transfer at 5 K, laser flashes (at a flash frequency of 5 Hz) from the MOPO 730 instrument (20 mJ at the sample position) of the desired wavelength were applied directly to the EPR cavity at 5 K. During the flash illumination, EPR spectra were continuously recorded, at approximately one spectrum per minute. After 10 min, the maximal amplitude of the split S_1 signal had been achieved. At this point, the laser flashing was interrupted and the EPR spectra of Chl_Z and Cyt b_{559} were recorded at 15 K within ∼15 min.

EPR Spectroscopy. Continuous wave (cw) EPR spectra were recorded with an ELEXSYS E500 spectrometer (Bruker Biospin) equipped with a SuperX bridge and a SHQ4122 cavity. All measurements were performed at a low temperature that was achieved with an Oxford Instrument cryostat and ITC-4 temperature controller. EPR spectra were analyzed with Bruker Xepr version 2.4b. EPR spectra from the split S_1 signals, oxidized Cytb_{559} (except for spectra from dark and 77 K illuminated samples), and Car/Chl radicals are presented as light minus dark difference spectra.

RESULTS

Oxidation of the Y_Z/$CaMn_4$ Pathway. We have monitored the far-red light-induced charge separation products in intact PS II-enriched membranes at 5 K. Figure 1A shows the results when PS II, synchronized in the S_1 state, was exposed to laser flashes with wavelengths ranging from 532 to 750 nm. Under these conditions, any formed $Y_Z^\bullet$ is observed via the so-called split S_1 EPR signal[39,48−54] that reflects a magnetic interaction between $Y_Z^\bullet$ and the $CaMn_4$ cluster. The appearance of the split S_1 EPR signal was analyzed at the amplitude of the peak in Figure 1A. It was found that Y_Z was oxidized to a large extent at 532 nm (spectrum a), 730 nm (spectrum b), and 740 nm (spectrum c). Quantification of the split S_1 EPR signal showed that Y_Z was oxidized in nearly 30% of PS II for these two far-red wavelengths and 40% of PS II for

dx.doi.org/10.1021/bi5006392 | *Biochemistry* 2014, 53, 4228−4238

532 nm (Table 1). Light at 750 nm (spectrum d) also clearly resulted in the formation of the split S_1 EPR signal. The amplitude was much lower and reflected ~8% of PS II (Table 1). Thus, oxidation of Y_Z at 5 K can be observed at least up to 750 nm.

Table 1. Charge Separation Products Induced at 5 K

λ (nm)	split S_1[a,d]	Cyt b_{559}[b,d]	Car/Chl radical[c,d]	total charge separation[e]	partition ratio[g]
532	40 (44)	35 (39)	15 (17)	90	0.8
730	27 (64)	13 (31)	2 (5)	42	1.8
740	27 (73)	10 (27)	0	37	2.7
750	8 (73)	<3[f] (<27)	0	11	>2.7

[a]Split S_1 EPR signal induction was quantified from the maximal inducible signal with white light, which has been shown to represent 40% of total PS II.[39,40] [b]Quantified from the integrated area of the peak at g_z = 3 compared to full oxidation of Cyt b_{559} with illumination at 77 K for 10 min.[57] [c]Quantified from comparison with the double integrated area of the nonsaturated EPR spectrum of $Y_D^•$ used as an internal standard ($Y_D^•$ has one radical per PS II center[42]). [d]Numbers in parentheses represent the percentage of total charge separation. Numbers without parentheses represent the percentage of total PS II. [e]In percent of PS II. [f]The EPR signal from oxidized Cyt b_{559} after illumination with light at 750 nm was too small to allow integration with any precision, and we estimate the signal to represent at maximum of 3% of the PS II centers. [g]The partition ratio is defined as (yield of Y_Z/$CaMn_4$ oxidation):(yield of Cyt b_{559}/Chl_Z/Car_{D2} oxidation).

This is to the best of our knowledge the first time oxidation of Y_Z driven by far-red light as low as 5 K has been observed in the S_1 state, and the reaction was overlooked in an earlier study by us[55] (see below for the Discussion). The induction and decay of this signal were therefore investigated further. Figure 1B shows the time-dependent increase in the amplitude of the split S_1 EPR signal during flashing at different wavelengths. As observed previously,[39,48,55] the induction was fast and efficient at 532 nm and reached its maximum within ~2 min of flashing at our laser power ($t_{1/2}$ ~ 53 s). The yield was approximately similar to that reached with continuous white light. The induction was equally fast at 730 nm but reached a lower amplitude. At 740 nm, the maximal amplitude was the same as that after 730 nm light flashing but was reached somewhat more slowly ($t_{1/2}$ ~ 69 s). The induction kinetics was again slower at 750 nm ($t_{1/2}$ ~ 85 s) where the maximal signal also was significantly smaller (see also Table 1).

We also followed the decay of the split S_1 signal when the laser flashing was turned off. Figure 1C shows the induction and decay of the signal induced by flashes at 730 nm. The amplitude of the signal decayed to ~70% of its original value with a decay half-time of 160 ± 5 s at this temperature. This behavior is normal for the split S_1 signal induced by visible light, which has been reported to decay via recombination with Q_A^- with a $t_{1/2}$ of ~3 min in the dominating part of the centers.[39,48,55] This also held for the split S_1 signal induced by 532 nm in this work, which also decayed with a $t_{1/2}$ of ~3 min (not shown).

Oxidation of the Cyt b_{559}/Chl_Z/Car_{D2} Pathway. Under conditions where donation of an electron from the $CaMn_4$ cluster is prohibited, the donation of a secondary electron to P_{680}^+ from the high-potential form of Cyt b_{559} or Chl_Z via Car_{D2} can occur (Scheme 1), resulting in stable charge pair Cyt $b_{559}^{ox}Q_A^-$ or $Chl_Z^+Q_A^-$.[31,38] The ratio between these mainly reflects the initial oxidation state of Cyt b_{559}. PS II membrane preparations always contain 20−30% the low-potential form of Cyt b_{559}, which is oxidized.[33,34] In this case, when Cyt b_{559} is oxidized in a PS II center prior to the illumination, the side path electron donation results in the formation of Chl_Z^+. Oxidation of both Cyt b_{559} and Chl_Z can be followed by EPR spectroscopy. Figure 2A displays the EPR spectra of oxidized Cyt b_{559}, achieved after flash illumination at 5 K. In our preparation, 30% of the total Cyt b_{559} is present in the oxidized low-potential form (Figure 2B, gray spectrum, and Table 1). The rest of Cyt b_{559} is the reduced high-potential form (70%) that can be observed after illumination at 77 K with white light (Figure 2B, black spectrum).

The signal induced at 532 nm and 5 K (Figure 2A, spectrum a) was large and reflects oxidation of Cyt b_{559} in its high-potential form, where g_z = 3.06.[34,56,57] It represented oxidation of Cyt b_{559} in 35% of PS II (Table 1). The level of Cyt b_{559} oxidation using 730, 740, or 750 nm light was much smaller (Figure 2A, spectra b−d). With 730 nm light, the amplitude of oxidized Cyt b_{559} was approximately one-third of that of the 532 nm-induced signal and reflected oxidation of Cyt b_{559} in

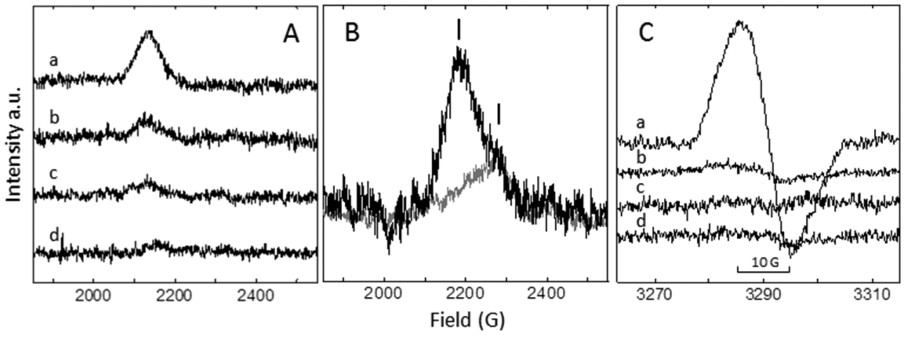

Figure 2. Wavelength-dependent induction of Cyt b_{559} and Chl_Z^+ in PS II. (A) Oxidation of Cyt b_{559} achieved by flash illumination at 5 K with 532 nm (spectrum a), 730 nm (spectrum b), 740 nm (spectrum c), and 750 nm (spectrum d) light. (B) Spectra from Cyt b_{559} in the dark-adapted samples (gray) and after illumination for 6 min at 77 K (black). Bars indicate the position of the low-potential form [g = 2.96 (right)] and high-potential form [g = 3.06 (left)] of Cyt b_{559} in the g_z region. EPR conditions: microwave frequency of 9.28 GHz, microwave power of 5 mW, modulation amplitude of 15 G, and temperature of 5 K. (C) Wavelength-dependent induction of Chl_Z^+ achieved by flash illumination at 5 K and 532 nm (spectrum a), 730 nm (spectrum b), 740 nm (spectrum c), and 750 nm (spectrum d). The spectra were deconvoluted as described in the Supporting Information, and the signal size was estimated on the basis of the $Y_D^•$ radical (one spin per PS II center[42]). EPR conditions: microwave frequency of 9.28 GHz, microwave power of 1.2 μW, modulation amplitude of 3.5 G, and temperature 15 K.

dx.doi.org/10.1021/bi5006392 | Biochemistry 2014, 53, 4228−4238

~13% of the PS II centers. With 740 nm light, the oxidation of Cyt b_{559} occurred in 10% of the PS II centers. With 750 nm light, the level of oxidation of Cyt b_{559} was even smaller. The EPR signal (Figure 2A, spectrum d) was too small to integrate, and we estimate it reflects oxidation of Cyt b_{559} in <3% of the PS II centers (Table 1).

Figure 2C shows the radical EPR spectra from Chl_Z^+ (10 G wide, g value of 2.0026)[57] induced by flash illumination at 5 K. The signal was deconvoluted to obtain clean Chl_Z^+ radical (see the Supporting Information). The amount of the induced radical was estimated via comparison of the fully oxidized Y_D radical (one spin per PS II reaction center[42]). At 532 nm, 15% of the Chl_Z^+ was formed (Figure 2C, spectrum a, and Table 1). Illumination at far-red wavelengths (730, 740, and 750 nm) did not result in any observable Chl_Z^+ formation (Figure 2C, spectra b–d, and Table 1). From these results, it is clear that the far-red light was not able to drive P_{680}^+ reduction with Cyt b_{559} or Chl_Z to any significant extent. In contrast, flashing with 532 nm light resulted in a significant oxidation of both Chl_Z and Cyt b_{559}, similar to what has been reported previously with white light.[39,41,48] However, both wavelength regimes could drive the $Y_Z/CaMn_4$ pathway, which could be observed as induction of the split S_1 EPR signal.

DISCUSSION

In intact PS II at room temperature, reduction of P_{680}^+ is completely dominated by the water oxidizing pathway. First, P_{680}^+ is reduced by Y_Z, which is thereafter reduced by an electron from the $CaMn_4$ cluster. At low temperatures, this changes and the transfer of an electron from the $CaMn_4$ complex to $Y_Z^\bullet$ is severely slowed or even completely inhibited. This is the situation at 5 K where P_{680}^+ partly is efficiently reduced by the Cyt $b_{559}/Chl_Z/Car_{D2}$ pathway. This electron donation pathway has been extensively studied and found to involve not only Cyt b_{559} and a chlorophyll donor that were discovered earlier[27,28,35,36] but also a carotenoid donor.[31,35−37,58,59] For a long time, the Cyt $b_{559}/Chl_Z/Car_{D2}$ pathway was thought to be the only functional pathway at 5 K and comparable low temperatures (there were no indications of Y_Z oxidation). However, the understanding of the low-temperature electron donation to P_{680}^+ changed with the discovery that split EPR signals, which originate from the $Y_Z^\bullet$ radical in magnetic interaction with the $CaMn_4$ cluster, could be induced at 5−10 K.[48,50,51,60] Thus, it became obvious that Y_Z could donate an electron to P_{680}^+ also at ultralow temperatures.[53,54] Both pathways also work and compete with each other at intermediate temperatures (77−273 K) where the temperature-dependent partition ratio between them was first studied.[29] It was found that at temperatures where the S_2-state multiline signal was not formed, Cyt b_{559} was oxidized instead.

With our observation that the photochemistry in PS II works with far-red illumination at room temperature,[15] it is also clear that the low-temperature photochemistry and secondary electron transfer reactions might be functional at these wavelengths to a higher degree than previously thought. In this work, we therefore applied EPR spectroscopy to investigate how the wavelength of the applied light affects the partition ratio between the electron donation from the $Y_Z/CaMn_4$ pathway and the Cyt $b_{559}/Chl_Z/Car_{D2}$ pathway.

Y_Z Oxidation after Far-Red Illumination at 5 K. Our results here show that the split S_1 EPR signal is formed in a considerable fraction of the PS II centers with illumination at least as high as 750 nm (Figure 1A and Table 1). This clearly demonstrates that Y_Z can be oxidized at 5 K following this low-energy illumination. Furthermore, our observation that the dominating part of the signal decayed via recombination with Q_A^- [$t_{1/2} \sim 3$ min at 5 K (Figure 1C)] shows that the oxidation of Y_Z is accompanied by reduction of Q_A. It thus occurs via charge separation between the donor and acceptor sides of PS II. This is in contrast to the split S_3 EPR signal that is formed via near-infrared (NIR)-induced excitation of the $CaMn_4$ cluster in the S_3 state and subsequent backward electron transfer from Y_Z to the $CaMn_4$ cluster. Consequently, because no Q_A^- is formed in the reaction, the split S_3 signal is stable at 5 K.[40,55]

We have earlier determined the formation spectra for the split S EPR signals. In this earlier work, we observed induction of the split S_3 signal at least to 900 nm while no formation of the split S_1 EPR signal was reported above 730 nm.[55] Our results here clearly extend the far-red limit for Y_Z oxidation in the S_1 state. There are two main reasons that we did not observe induction of the split S_1 signal after far-red illumination in our earlier work.[55] The MOPO laser flash source available was significantly weaker and less stable than the system presented here. In addition, the signal-to-noise level was 3−4 times lower in the EPR spectrometer than in our present instrument. Taken together, these two factors pressed the obtainable spectrum into the noise level of the measurement; it thus escaped our attention. Scrutiny of our old spectra indeed reveals the presence of the split S_1 signal just above the noise level (not shown), too small to allow clear identification at that time.[55]

Partition Ratio between Electron Donor Pathways in PS II. The first attempt to define the degree to which Y_Z could be oxidized at 5 K was conducted in the S_0 state.[48] This study was done by comparison with the amplitude of the split signal in Ca-depleted PS II, and it was found that the split S_0 signal (where this particular comparison was best applicable) was formed in ~40% of PS II centers that were in the S_0 state. The same fraction of Y_Z oxidation also occurred in the S_1 state in PS II both from *Spinacia oleracea* (spinach) and from *Thermosynechococcus elongates* (cyanobacteria). This was found in a study of the split S_1 EPR signal where both electron donors and acceptors were quantified by EPR.[39] Similar studies have now been performed in the S_3 state,[40] and it is generally accepted that at 5 K using visible light illumination, P_{680}^+ is reduced from either the $Y_Z/CaMn_4$ pathway or the Cyt $b_{559}/Chl_Z/Car_{D2}$ pathway in an approximate partition ratio of 1.[a]

This partition ratio is thought to reflect a molecular heterogeneity around Y_Z. In one configuration, Y_Z can reduce P_{680}^+ efficiently, while in another configuration, it is unable to compete with the Cyt $b_{559}/Chl_Z/Car_{D2}$ pathway to reduce P_{680}^+. It has been pointed out that such heterogeneity is likely to exist also at room temperature, resulting in different kinetics for Y_Z oxidation by P_{680}^+,[39,61,62] although these kinetics are always fast enough to outcompete the donation of an electron from the Cyt $b_{559}/Chl_Z/Car_{D2}$ pathway. The heterogeneity is likely to be locked in by freezing of the sample to temperatures as low as 5 K, where hardly any movement of the protein is possible.

In this study, we found that 44% of the formed P_{680}^+ is reduced from the $Y_Z/CaMn_4$ pathway and 56% is reduced from the Cyt $b_{559}/Chl_Z/Car_{D2}$ pathway, resulting in a partition ratio of 0.8 when light at 532 nm was used to drive the charge separation (Figure 3A and 3B). This is quite similar to what was found with white light in ref 39 and confirms that our samples

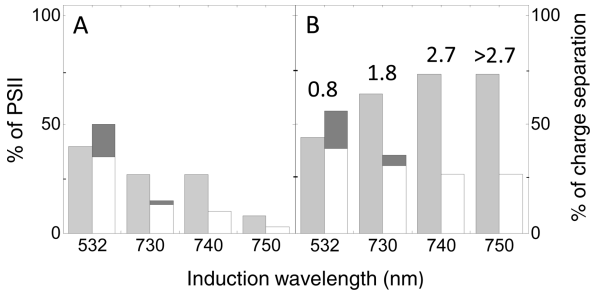

Figure 3. Oxidation of electron donors to P_{680}^+ by illumination at 5 K. (A) Result of flash illumination at different wavelengths. The bars represent formation of the split S_1 signal (gray), oxidation of Cyt b_{559} (white), and oxidation of Chl_Z (dark gray) as a percent of total PS II. The data are from Table 1. (B) Oxidation of the different electron donors as a fraction of the total stable charge separation achieved at the specific excitation wavelength: Y_Z oxidation (gray bars), Cyt b_{559} oxidation (white bars), and Chl_Z oxidation (dark gray bars). The partition ratio between the $Y_Z/CaMn_4$ and Cyt $b_{559}/Chl_Z/Car_{D2}$ pathways is also shown.

behaved similarly. Thus, in ∼44% of PS II, Y_Z is in a configuration that allows efficient transfer of an electron to P_{680}^+. In the remaining fraction of PS II, Y_Z is in a configuration that either does not allow Y_Z oxidation at 5 K or, alternatively, slows Y_Z oxidation enough to permit the Cyt $b_{559}/Chl_Z/Car_{D2}$ pathway to win the competition. In either case, the situation around Y_Z should be the same in all our PS II samples that are treated in exactly the same way before illumination. After the samples had been frozen to 5 K, the situation should be set and every time P_{680}^+ is formed in a reaction center Y_Z should be able to donate an electron in 44% of the cases.

This is clearly not the case when PS II is exposed to monochromatic >730 nm light (Figure 3A). At 730 nm, the total amount of stable charge separation products we observed represented 42% of the PS II centers (Table 1). $Y_Z^\bullet$ formation occurred in 27% and Cyt b_{559} oxidation in 13% of PS II, while we could observe oxidation of Chl_Z or Car_{D2} in only 2% of PS II (Figure 3A and Table 1). This results in a partition ratio of 1.8 between the two pathways. At 740 nm, the partition ratio was 2.7 (Table 1 and Figure 3B), which is significantly higher. Here the EPR spectra from the split S_1 signal and oxidized Cyt b_{559} were sufficiently large to allow precise quantification. At 750 nm, the yield of respective donors was smaller, making quantification of, in particular, the Cyt b_{559} spectrum less precise. Here the partition ratio was 2.5−3 (>2.7). Thus, the trend is that the higher the excitation wavelength, the lower the probability the oxidized primary donor has to oxidize the Cyt $b_{559}/Chl_Z/Car_{D2}$ pathway. Following illumination at >740 nm, the oxidized primary donor is reduced by Y_Z in ∼75% of the PS II centers that underwent charge separation (Table 1).

An important question is if this effect is a general property of PS II or is preparation-dependent and somehow reflects the purity or integrity of the PS II complex. It is known that even in very similar preparations, slight differences in, for example, the detergent treatment sometimes can induce heterogeneity in the protein and antenna composition and affect the redox properties, especially on the acceptor side of PS II. Our experiments described above were performed in a PS II-enriched membrane preparation with milder stacking and detergent treatments,[43] which allows high oscillation of the OEC than more often used preparations.[40,47] We therefore performed similar experiments in the standard type BBY preparation with a harder stacked thylakoid membrane and prolonged detergent treatment.[44−46] The results are listed in Table 2. The partition ratios between the two donor pathways obtained for 535 and 740 nm illumination were remarkably similar in both preparations.

Thus, this discrimination against the Cyt $b_{559}/Chl_Z/Car$ pathway following excitation with far-red light is an interesting property of the PS II complex, and below we will present our hypothesis to explain this phenomenon.

Location of the First Oxidized Primary Donor after Far-Red Illumination. The question of why the far-red light cannot drive the Cyt $b_{559}/Chl_Z/Car_{D2}$ pathway as well as the $Y_Z/CaMn_4$ pathway at 5 K now arises. To discuss this, we point out that PS II in our study is frozen at 5 K. At this extremely low temperature, only very minor atomic movements will occur in the protein and all molecular properties in the reaction center that have been frozen in will remain until the sample is thawed to a much higher temperature. An example of such heterogeneity is the exact location of the phenolic proton on Y_Z in the hydrogen bonding network in which it participates. In case the proton is located and/or frozen in close to the phenolic oxygen proton, Y_Z might be difficult to oxidize at 5 K because this would require significant proton movement. In case the proton is instead frozen in closer to the proton acceptor(s), Y_Z might be easy to oxidize also at 5 K. This type of frozen-in heterogeneity is likely to explain the Y_Z oxidation ratio (in ∼40% of PS II) that is reported at 5 K[39,40] (see also Table 1). However, this type of frozen-in heterogeneity will not change between our samples that are all treated similarly before they are frozen to 5 K. The same type of consideration also holds for possible molecular differences around the chlorin pigments in the PS II core [$Pheo_{D1}$, $Pheo_{D2}$, Chl_{D1}, Chl_{D2}, P_{D1}, and P_{D2} (Scheme 1 and Figure 4)] and the redox components in the Cyt $b_{559}/Chl_Z/Car_{D2}$ pathway. Also, such differences would be similar in all samples, and we have difficulty in

Table 2. Properties and Partition Ratios of Two PS II Membrane Preparations Used in This Work

PS II[a] preparation	Triton[b] X-100 treatment	PS I[c] content (%)	Chl *a*/*b*	no.[d] of Chls per PS II	O_2[e] evolution	partition[f] ratio at 532 nm	partition[f] ratio at 740 nm
prepatation A	20 min	8	2.3	236	370	0.8	2.7
preparation B	30 min	<3	2.1	205	440	0.8	2.6

[a]The preparation used in most experiments in this study was preparation A. Preparation B (BBY type) was used to check the partition ratio in a "standard" preparation of PS II-enriched membranes. [b]The detergent treatment step during the preparation included incubation in the presence of Triton X-100 (25 mg/mg of Chl) for 20 min in procedure A and for 30 min (after the additional thylakoid stacking step) in procedure B. [c]PS I was quantified from the P_{700}^+ radical and induced by chemical oxidation with 10 mM ferricyanide, in comparison to the spectrum of fully oxidized $Y_D^\bullet$, which was used as an internal standard.[42] [d]Estimated by comparison to the doubly integrated size of the $Y_D^\bullet$ radical in thylakoid membranes (380 Chls/PS II center[78]) and in the preparations of PS II-enriched membranes from spinach. [e]Oxygen evolution was measured with an electrode at 20 °C with 0.5 mM PpBQ as the electron acceptor under saturating white light illumination. [f]The partition ratio is defined as in Table 1[a].

dx.doi.org/10.1021/bi5006392 | *Biochemistry* 2014, 53, 4228−4238

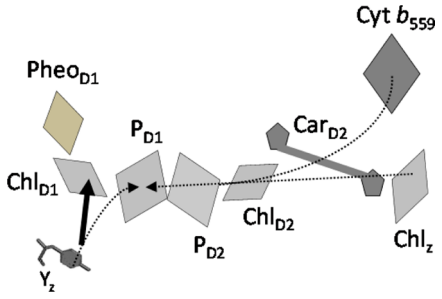

Figure 4. Schematic representation of the pigments in P_{680} and the redox components in the Y_Z/$CaMn_4$ and Cyt b_{559}/Chl_Z/Car_{D2} pathways. The dotted arrows represent the electron transfer reactions following illumination with visible light at 5 K. The solid arrow represents the suggested dominating primary electron transfer after far-red illumination at 5 K between Chl_{D1} and Y_Z.

determining a mechanism at 5 K by which the excitation wavelength would steer the molecular configurations around PS II redox components.

Instead, we argue that the different partition ratios observed between visible and far-red light excitation should be sought in the product formed by the excitation and primary charge separation. Excitation of P_{680} with green light results in primary charge separation pair $P_{680}^{+}Q_A^{-}$, where the electron hole is located to P_{D1} creating charge pair $P_{D1}^{+}Q_A^{-}$[8,21,63−66] (Figure 4). We propose here that far-red light at 5 K excites a different component here denoted P_x (denoted X at room temperature in ref 15). Excitation of P_x then leads to the formation of the first stable charge pair $P_x^{+}Q_A^{-}$. To explain our results, we suggest that this is spatially and/or energetically different from the $P_{D1}^{+}Q_A^{-}$ charge pair induced with green light. P_{D1} is one of the chlorophylls in P_{680} and is bound to the D_1 protein. It is located close to Y_Z [9 Å, edge to edge (Table 3)], which allows

Table 3. Distances between Pigments and Redox Components on the Donor Side of PS II[a]

pigments	distance (Å)
$Y_Z \rightarrow P_{D1}$	9.4
$Y_Z \rightarrow P_{D2}$	16.8
$Y_Z \rightarrow Chl_{D1}$	11.3
$Y_Z \rightarrow Chl_{D2}$	19.8
$Car_{D2} \rightarrow P_{D1}$	22.0
$Car_{D2} \rightarrow P_{D2}$	23.7
$Car_{D2} \rightarrow Chl_{D1}$	28.8
$Car_{D2} \rightarrow Chl_{D2}$	11.3

[a]Distances reflect the shortest edge-to-edge distance in the PS II structure from ref 16.

fast electron donation occurring from Y_Z in the nanosecond time regime at room temperature. Donation of an electron from Y_Z is also efficient at 5 K and dominates in centers where the frozen-in configuration around Y_Z allows its oxidation. P_{D1} is seemingly also situated sufficiently close to Car_{D2} [closest edge-to-edge distance of 22 Å (Table 3)] to allow its oxidation when Y_Z is unable to deliver an electron fast. This is then followed by the transfer of an electron from Chl_Z or Cyt b_{559} to oxidized Car_{D2}.

Our results show that far-red illumination preferentially leads to oxidation of the Y_Z/$CaMn_4$ pathway while the Cyt b_{559}/Chl_Z/Car_{D2} pathway is almost isolated from the oxidized primary donor at 5 K (Figure 3B, partition ratios, and Table 1). There could be several reasons for this. Photons in the far-red region contain less energy than photons in the visible region. It is therefore tempting to suggest that far-red species of the oxidized primary donor (P_X) also could have a lower energy content, i.e., be less oxidizing after far-red oxidation, and that this would alter the partition ratio between the two pathways. P_X should in this case have problems oxidizing Y_Z and instead preferentially receive its electron from the more easily oxidized Car_{D2} (~785 mV *in vitro*[67]) if the electron hole was located on the same component as after visible light illumination (P_{D1}). We find this to be an unlikely explanation for our results because Y_Z oxidation is actually preferred. Thus, the oxidation potential for Y_Z (~1.2 V[25]) is clearly achieved.

Instead, we propose that the electron hole after far-red excitation is located on a component different from P_{D1}. This should be farther from Car_{D2} than P_{D1} to render Car_{D2} and subsequent Cyt b_{559}/Chl_Z oxidation an unlikely event at low temperatures. It should, however, be situated close enough to Y_Z to allow its oxidation at 5 K. A model for this is schematically illustrated in Figure 4. P_{D2} is much farther from Y_Z (17 Å) than P_{D1} (9 Å) (Table 2); this also holds for Chl_{D2} (20 Å from Y_Z). Their distances to Car_{D2} are similar to (24 Å) or much shorter than the P_{D1}−Car_{D2} distance of 22 Å (11 Å) (Table 2). Consequently, they are unlikely candidates for P_X because their oxidation by far-red light would result in oxidation of the Cyt b_{559}/Chl_Z/Car_{D2} pathway similar to P_{D1}^{+} oxidation. This is contrary to our findings.

Therefore, we suggest that the charge separation under far-red illumination leads to oxidation of Chl_{D1} by $Pheo_{D1}$ (Figure 4). Of the four chlorophylls in the P_{680} ensemble, this is farthest from Car_{D2} [29 Å, edge to edge (Table 3)]. It is, however, situated only 11 Å from Y_Z, clearly close enough to permit efficient electron transfer from Y_Z. Thus, if Chl_{D1}^{+} is the dominating species formed by far-red light, this would most likely strongly favor oxidation of the Y_Z/$CaMn_4$ pathway over the Cyt b_{559}/Chl_Z/Car_{D2} pathway.

Both Chl_{D1}^{+} and P_{D1}^{+} have been assigned to be the first cationic species formed in the early steps during primary charge separation.[6,8,68,69] A combination of these acting together was also proposed.[20] Regardless of where it is formed, the electron hole is proposed to migrate to P_{D1} and end there via rapid charge equilibrium between the reaction center pigments.[8] Our results indicate that this probably holds at 5 K after visible light illumination (532 nm) where the "normal" product P_{D1}^{+} most probably is the dominating product. If electron hole migration also occurred when PS II is illuminated with far-red light at 5 K, both illumination regimes would create the same stable cation, P_{D1}^{+}. This contradicts the wavelength-dependent partition ratios determined here (Figure 3B and Table 1). Instead, our results indicate that the cation formed after primary charge separation is located differently after far-red illumination. This suggests that the electron hole does not equilibrate between the pigments at 5 K, at least when the charge separation is triggered by far-red light. Instead of ending up at P_{D1}, the electron hole ends up at Chl_{D1}.

If this conclusion proves to be correct, it implies that the charge equilibrium between Chl_{D1} and P_{D1} ($Chl_{D1}^{+}P_{D1} \rightleftharpoons Chl_{D1}P_{D1}^{+}$) is strongly inhibited at 5 K. Therefore, Chl_{D1}^{+} seems to be excluded as one of the participating species leading to P_{D1}^{+} formation when PS II photochemistry is investigated at 5 K in intact, oxygen-evolving PS II. In this respect, it is important that most studies indicating efficient charge equilibria involving species assigned to Chl_{D1} have been performed at

dx.doi.org/10.1021/bi5006392 | *Biochemistry* 2014, 53, 4228−4238

≥77 K.[20,64,68] The studies have sometimes also been restricted to the D_1/D_2/Cyt b_{559} reaction center preparation.[20] This is quite different from our experiment described here. In particular, the difference in the PS II preparations used is very important because the D_1/D_2/Cyt b_{559} reaction center preparation lacks (in addition to the entire antenna complex) the quinone electron acceptors and more importantly the $CaMn_4$ cluster and functional Y_Z and Y_D.[70]

Identity of the Far-Red-Absorbing Pigments. An interesting question is also the identity of the far-red light-absorbing pigment(s) in Photosystem II that can drive both primary and secondary charge separation. The different charge separation products we observe between 532 nm and far-red light excitation strongly indicate that the charge separation is performed with the provided excitation energy. This is expected at 5 K and shows that no uphill energy transfer process is involved. Antenna absorption occurring in the far-red region at 5 K can probably be ruled out because the outer antennas (light-harvesting complex II) in PS II have no absorption above 678 nm[71−73] while the absorption limit for the inner antenna is at 703 nm at 1.7 K for the CP 47 subunit.[13] It is therefore probable that the far-red-absorbing pigments are located in the reaction center assembly itself where four chlorophylls and two pheophytins (Scheme 1 and Table 3) are densely packed and excitonically coupled.[17,69,74]

It is tempting to compare with the so-called red Chls in the outer antennas subunits of PS I. These are a chlorophyll dimer that has an absorption maximum between 705 and 710 nm resulting from strong excitonic coupling and orbital overlap between the two chlorophylls.[75] These two features facilitate the far-red absorption and the large Stokes shift that characterize their low-temperature fluorescence emission. The tight packing of pigments in the PS II reaction center is not too dissimilar. It is therefore not surprising that similarities in the excited state of the reaction center pigments of PS II (P_{D1}, P_{D2}, Chl_{D1}, and $Pheo_{D1}$) and the red chlorophylls recently were demonstrated by Stark spectroscopy.[66,76,77] The excited state of these pigments had a mixed exciton charge transfer (CT) character. The presence of a CT state in the reaction center responsible for the far-red absorption was previously suggested,[13,74] but the long wavelength absorption properties of the charge transfer band could in those studies not be directly probed. Instead, it was observed as changes in the Stark spectrum around 680 nm.[66]

So far, these charge transfer bands have been reported or suggested up to 730 nm,[13,74] but it is not unlikely that new states with higher absorption maxima can be discovered when spectroscopic techniques and sample preparation have advanced further. The charge transfer states giving rise to the absorption between 700 and 730 nm probably derive from the coupling between Chl_{D1} and $Pheo_{D1}$ or between P_{D1} and P_{D2}.[66] However, these pairs are unlikely to be the only possible pigment combinations that can give rise to states of this charge transfer type. Instead, we propose that the far-red-induced photochemistry we describe here is driven by a hitherto unidentified, redox active charge transfer state formed between two or more of the tightly packed pigments in the PS II reaction center core. One of these is likely to be Chl_{D1}, which we propose is the carrier of the electron hole, P_X^+, which is formed after far-red light triggered charge separation at 5 K. There are different candidates for the interacting species, and its identification will demand very precise optical studies in fully active PS II preparations in contrast to the spectroscopically more accessible D_1/D_2/Cyt b_{559} reaction center preparation used in refs 20 and 66, for example.

CONCLUSIONS

On the basis of our results, we suggest that PS II has a second previously unknown charge separation pathway. We show a difference in the charge separation product ratio between 532 nm and far-red light flash illumination at a cryogenic temperature (5 K). The deviation is suggested to depend on the formation of a first stable charge pair different from the visible light-induced $P_{D1}^+Q_a^-$ charge pair. We denote this state $P_x^+Q_a^-$. P_x^+ is most probably formed by the absorption of two or more closely interacting porphyrin pigments (chlorophyll and/or pheophytin) in the PS II reaction center core. The existence of such a state has indeed been suggested previously[13,66,74] but never shown to induce charge separation at wavelengths as high as 750 nm at cryogenic temperatures until this study. We also propose that the electron hole in P_x^+ is residing on the Chl_{D1} molecule at 5 K. This would explain that far-red illumination preferentially drives efficient electron transfer from Y_Z while we observe only very weak oxidation of the Cyt $b_{559}/Chl_Z/Car_{D2}$ pathway.

ASSOCIATED CONTENT

Supporting Information

Additional observations and wavelength-dependent induction of radical EPR signals at 5 K in PS II-enriched membranes (Figure 1). This material is available free of charge via the Internet at http://pubs.acs.org.

AUTHOR INFORMATION

Corresponding Author

*Phone: +46 18 471 6580. Fax: +46 471 6844. E-mail: stenbjorn.styring@kemi.uu.se.

Funding

The Swedish Research Council, the Swedish Energy Agency, and the Knut and Alice Wallenberg Foundation are gratefully acknowledged for financial support.

Notes

The authors declare no competing financial interest.

ACKNOWLEDGMENTS

We also thank Prof. Rienk van Grondelle for useful discussions.

ABBREVIATIONS

Car, carotenoid; Chl, chlorophyll; Cyt b_{559}, cytochrome b_{559}; D1 and D2, core protein subunits in PS II; EPR, electron paramagnetic resonance; MES, 2-(*N*-morpholino)-ethanesulfonic acid; P_{680}, primary electron donor in PS II; P_{700}, primary electron donor in PS I; Pheo, pheophytin; PS I, Photosystem I; PS II, Photosystem II; Q_A and Q_B, primary and secondary quinone acceptors, respectively, in PS II; Y_Z and Y_D, redox active tyrosines in PS II.

ADDITIONAL NOTE

[a]We define in this work a partition ratio between the electron donor pathways in PS II. The partition ratio equals (yield of $Y_Z/CaMn_4$ oxidation):(yield of Cyt $b_{559}/Chl_Z/Car_{D2}$ oxidation).

REFERENCES

(1) Blankenship, R. E. (2008) *Molecular mechanisms of photosynthesis*, Wiley-Blackwell, New York.

(2) Emerson, R., and Lewis, C. M. (1943) The dependence of the quantum yield of *Chlorella* photosynthesis on wavelength of light. *Am. J. Bot. 30*, 165−178.

(3) Emerson, R., Chalmers, R., and Cederstrand, C. (1957) Some factors influencing the long-wave limit of photosynthesis. *Proc. Natl. Acad. Sci. U.S.A. 43*, 133−143.

(4) Duysens, L. N., Kamp, B. M., and Amesz, J. (1961) Two photochemical systems in photosynthesis. *Nature 190*, 510−511.

(5) Doring, G., Stiehl, H. H., and Witt, H. T. (1967) A 2nd chlorophyll reaction in electron chain of photosynthesis: Registration by repetitive excitation technique. *Z. Naturforsch., B: J. Chem. Sci. 22*, 639.

(6) Dekker, J. P., and van Grondelle, R. (2000) Primary charge separation in Photosystem II. *Photosynth. Res. 63*, 195−208.

(7) Barber, J., and Archer, M. D. (2001) P680, the primary electron donor of photosystem II. *J. Photochem. Photobiol., A 142*, 97−106.

(8) Cardona, T., Sedoud, A., Cox, N., and Rutherford, A. W. (2012) Charge separation in Photosystem II: A comparative and evolutionary overview. *Biochim. Biophys. Acta 1817*, 26−43.

(9) Renger, G. (2008) Functional Pattern of Photosystem II. In *Primary Processes of Photosynthesis. Part 2: Principles and Apparatus*, pp 237−290, The Royal Society of Chemistry, London.

(10) Greenbaum, N. L., and Mauzerall, D. (1991) Effect of irradiance level on distribution of chlorophylls between PS II and PS I as determined from optical cross-sections. *Biochim. Biophys. Acta 1057*, 195−207.

(11) Pettai, H., Oja, V., Freiberg, A., and Laisk, A. (2005) Photosynthetic activity of far-red light in green plants. *Biochim. Biophys. Acta 1708*, 311−321.

(12) Peterson-Årsköld, S., Masters, V. M., Prince, B. J., Smith, P. J., Pace, R. J., and Krausz, E. (2003) Optical spectra of *Synechocystis* and spinach Photosystem II preparations at 1.7 K: Identification of the D1-pheophytin energies and Stark shifts. *J. Am. Chem. Soc. 125*, 13063−13074.

(13) Hughes, J. L., Smith, P., Pace, R., and Krausz, E. (2006) Charge separation in photosystem II core complexes induced by 690−730 nm excitation at 1.7 K. *Biochim. Biophys. Acta 1757*, 841−851.

(14) Hughes, J. L., Krausz, E., Smith, P. J., Pace, R. J., and Riesen, H. (2005) Probing the lowest energy chlorophyll a states of Photosystem II via selective spectroscopy: New insights on P680. *Photosynth. Res. 84*, 93−98.

(15) Thapper, A., Mamedov, F., Mokvist, F., Hammarström, L., and Styring, S. (2009) Defining the far-red limit of Photosystem II in spinach. *Plant Cell 21*, 2391−2401.

(16) Umena, Y., Kawakami, K., Shen, J.-R., and Kamiya, N. (2011) Crystal structure of oxygen-evolving photosystem II at a resolution of 1.9 Å. *Nature 473*, 55−60.

(17) Durrant, J. R., Klug, D. R., Kwa, S. L. S., van Grondelle, R., Porter, G., and Dekker, J. P. (1995) A multimer model for P_{680}, the primary electron-donor of Photosystem II. *Proc. Natl. Acad. Sci. U.S.A. 92*, 4798−4802.

(18) Boxer, S. G., Goldstein, R. A., Lockhart, D. J., Middendorf, T. R., and Takiff, L. (1989) Excited-states, electron-transfer reactions, and intermediates in bacterial photosynthetic reaction centers. *J. Phys. Chem. 93*, 8280−8294.

(19) Middendorf, T. R., Mazzola, L. T., Lao, K. Q., Steffen, M. A., and Boxer, S. G. (1993) Stark-effect (electroabsorption) spectroscopy of photosynthetic reaction centers at 1.5 K: Evidence that the special pair has a large excited-state polarizability. *Biochim. Biophys. Acta 1143*, 223−234.

(20) Romero, E., van Stokkum, I. H. M., Novoderezhkin, V. I., Dekker, J. P., and van Grondelle, R. (2010) Two different charge separation pathways in photosystem II. *Biochemistry 49*, 4300−4307.

(21) Diner, B. A., Schlodder, E., Nixon, P. J., Coleman, W. J., Rappaport, F., Lavergne, J., Vermaas, W. F. J., and Chisholm, D. A. (2001) Site-directed mutations at D1-His198 and D2-His 97 of photosystem II in *Synechocystis* PCC 6803: Sites of primary charge separation and cation and triplet stabilization. *Biochemistry 40*, 9265−9281.

(22) Messinger, J., and Renger, G. (2008) Photosynthetic Water Splitting. In *Primary Processes of Photosynthesis. Part 2: Principles and Apparatus*, pp 291−349, The Royal Society of Chemistry, London.

(23) Kok, B., Forbush, B., and McGloin, M. (1970) Cooperation of charges in photosynthetic O_2 evolution-I. A linear four step mechanism. *Photochem. Photobiol. 11*, 457−475.

(24) Styring, S., and Rutherford, A. W. (1987) In the oxygen-evolving complex of photosystem II the S_0 state is oxidized to the S_1 state by D^+ (Signal-II_{slow}). *Biochemistry 26*, 2401−2405.

(25) Grabolle, M., and Dau, H. (2005) Energetics of primary and secondary electron transfer in Photosystem II membrane particles of spinach revisited on basis of recombination-fluorescence measurements. *Biochim. Biophys. Acta 1708*, 209−218.

(26) Rappaport, F., and Diner, B. A. (2008) Primary photochemistry and energetics leading to the oxidation of the $(Mn)_4Ca$ cluster and to the evolution of molecular oxygen in Photosystem II. *Coord. Chem. Rev. 252*, 259−272.

(27) Knaff, D. B., and Arnon, D. I. (1969) Spectral evidence for a new photoreactive component of oxygen-evolving system in photosynthesis. *Proc. Natl. Acad. Sci. U.S.A. 63*, 963−969.

(28) Knaff, D. B., and Arnon, D. I. (1969) Light-induced oxidation of a chloroplast b-type cytochrome at −189 °C. *Proc. Natl. Acad. Sci. U.S.A. 63*, 956−962.

(29) Thompson, L. K., and Brudvig, G. W. (1988) Cytochrome b_{559} may function to protect Photosystem II from photoinhibition. *Biochemistry 27*, 6653−6658.

(30) Thompson, L. K., Miller, A. F., Buser, C. A., de Paula, J. C., and Brudvig, G. W. (1989) Characterization of the multiple forms of cytochrome b_{559} in photosystem II. *Biochemistry 28*, 8048−8056.

(31) Hanley, J., Deligiannakis, Y., Pascal, A., Faller, P., and Rutherford, A. W. (1999) Carotenoid oxidation in photosystem II. *Biochemistry 38*, 8189−8195.

(32) Magnuson, A., Rova, M., Mamedov, F., Fredriksson, P.-O., and Styring, S. (1999) The role of cytochrome b_{559} and $tyrosine_D$ in protection against photoinhibition during in vivo photoactivation of photosystem II. *Biochim. Biophys. Acta 1411*, 180−191.

(33) Faller, P., Fufezan, C., and Rutherford, A. W. (2005) Side-path electron donors: Cytochrome b_{559}, $chlorophyll_z$ and β-carotene. In *Photosystem II. The Light-Driven Water:Plastoquinone Oxidoreductase* (Wydrzynski, T. J., Satoh, K., and Freeman, J. A., Eds.) Springer, Dordrecht, The Netherlands.

(34) Stewart, D. H., and Brudvig, G. W. (1998) Cytochrome b_{559} of photosystem II. *Biochim. Biophys. Acta 1367*, 63−87.

(35) Visser, J. W. M., Rijgersberg, C. P., and Gast, P. (1977) Photooxidation of chlorophyll in spinach chloroplasts between 10 and 180 K. *Biochim. Biophys. Acta 460*, 36−46.

(36) Vermeglio, A., and Mathis, P. (1973) Photooxidation of cytochrome b_{559} and electron donors in chloroplast Photosystem II. *Biochim. Biophys. Acta 292*, 763−771.

(37) Vrettos, J. S., Stewart, D. H., de Paula, J. C., and Brudvig, G. W. (1999) Low-temperature optical and resonance Raman spectra of a carotenoid cation radical in photosystem II. *J. Phys. Chem. B 103*, 6403−6406.

(38) Tracewell, C. A., Cua, A., Stewart, D. H., Bocian, D. F., and Brudvig, G. W. (2001) Characterization of carotenoid and chlorophyll photooxidation in photosystem II. *Biochemistry 40*, 193−203.

(39) Zhang, C., Boussac, A., and Rutherford, A. W. (2004) Low-temperature electron transfer in photosystem II: A tyrosyl radical and semiquinone charge pair. *Biochemistry 43*, 13787−13795.

(40) Havelius, K. G. V., Su, J.-H., Han, G., Mamedov, F., Ho, F. M., and Styring, S. (2011) The formation of the split EPR signal from the S_3 state of photosystem II does not involve primary charge separation. *Biochim. Biophys. Acta 1807*, 11−21.

(41) Sjöholm, J., Havelius, K. G. V., Mamedov, F., and Styring, S. (2009) The S_0 state of the water oxidizing complex in Photosystem II:

pH dependence of the EPR split signal induction and mechanistic implications. *Biochemistry 48*, 9393−9404.
(42) Danielsson, R., Albertsson, P.-Å., Mamedov, F., and Styring, S. (2004) Quantification of photosystem I and II in different parts of the thylakoid membrane from spinach. *Biochim. Biophys. Acta 1608*, 53−61.
(43) Völker, M., Ono, T., Inoue, Y., and Renger, G. (1985) Effect of trypsin on PS II particles: Correlation between Hill-activity, Mn-abundance and peptide pattern. *Biochim. Biophys. Acta 806*, 25−34.
(44) Berthold, D. A., Babcock, G. T., and Yocum, C. F. (1981) A highly resolved, oxygen-evolving photosystem II preparation from spinach thylakoid membranes. *FEBS Lett. 134*, 231−234.
(45) Ford, R. C., and Evans, M. C. W. (1983) Isolation of photosystem 2 preparation from higher plants with highly enriched oxygen evolving activity. *FEBS Lett. 160*, 159−164.
(46) Franzen, L.-E., Hansson, O., and Andreasson, L.-E. (1985) The roles of the extrinsic subunits in Photosystem II as revealed by EPR. *Biochim. Biophys. Acta 808*, 171−179.
(47) Han, G. Y., Mamedov, F., and Styring, S. (2012) Misses during water oxidation in photosystem II are S state-dependent. *J. Biol. Chem. 287*, 13422−13429.
(48) Zhang, C. X., and Styring, S. (2003) Formation of split electron paramagnetic resonance signals in photosystem II suggests that tyrosine$_z$ can be photooxidized at 5 K in the S_0 and S_1 states of the oxygen-evolving complex. *Biochemistry 42*, 8066−8076.
(49) Sjöholm, J., Styring, S., Havelius, K. G. V., and Ho, F. M. (2012) Visible light induction of an electron paramagnetic resonance split signal in Photosystem II in the S_2 state reveals the importance of charges in the oxygen-evolving center during catalysis: A unifying model. *Biochemistry 51*, 2054−2064.
(50) Ioannidis, N., and Petrouleas, V. (2000) Electron paramagnetic resonance signals from the S_3 state of the oxygen-evolving complex. A broadened radical signal induced by low-temperature near-infrared light illumination. *Biochemistry 39*, 5246−5254.
(51) Nugent, J. H. A., Turconi, S., and Evans, M. C. W. (1997) EPR investigation of water oxidizing photosystem II: Detection of new EPR signals at cryogenic temperatures. *Biochemistry 36*, 7086−7096.
(52) Koulougliotis, D., Teutlolf, C., Sanakis, Y., Lubitz, W., and Petrouleas, V. (2004) The S_1Y_Z·metalloradical intermediate in photosystem II: An X- and W-band EPR study. *Phys. Chem. Chem. Phys. 6*, 4859−4863.
(53) Havelius, K. G. V., Sjöholm, J., Ho, F. M., Mamedov, F., and Styring, S. (2010) Metalloradical EPR signals from the $Y_Z^{\bullet}$ S-state intermediates in photosystem II. *Appl. Magn. Reson. 37*, 151−176.
(54) Petrouleas, V., Koulougliotis, D., and Ioannidis, N. (2005) Trapping of metalloradical intermediates of the S-states at liquid helium temperatures. Overview of the phenomenology and mechanistic implications. *Biochemistry 44*, 6723−6728.
(55) Su, J.-H., Havelius, K. G. V., Ho, F. M., Han, G., Mamedov, F., and Styring, S. (2007) Formation spectra of the EPR split signals from the S_0, S_1, and S_3 states in photosystem II induced by monochromatic light at 5 K. *Biochemistry 46*, 10703−10712.
(56) Mamedov, F., Danielsson, R., Gadjieva, R., Albertsson, P.-A., and Styring, S. (2008) EPR characterization of photosystem II from different domains of the thylakoid membrane. *Biochemistry 47*, 3883−3891.
(57) Miller, A.-F., and Brudvig, G. W. (1991) A guide to electron paramagnetic resonance spectroscopy of photosystem II membranes. *Biochim. Biophys. Acta 1056*, 1−18.
(58) Tracewell, C. A., Vrettos, J. S., Bautista, J. A., Frank, H. A., and Brudvig, G. W. (2001) Carotenoid photooxidation in photosystem II. *Arch. Biochem. Biophys. 385*, 61−69.
(59) Faller, P., Maly, T., Rutherford, A. W., and MacMillan, F. (2001) Chlorophyll and carotenoid radicals in photosystem II studied by pulsed ENDOR. *Biochemistry 40*, 320−326.
(60) Nugent, J. H., Muhiuddin, I. P., and Evans, M. C. (2002) Electron transfer from the water oxidizing complex at cryogenic temperatures: The S_1 to S_2 step. *Biochemistry 41*, 4117−4126.
(61) Chen, G. Y., Han, G. Y., Göransson, E., Mamedov, F., and Styring, S. (2012) Stability of the S_3 and S_2 state intermediates in photosystem II directly probed by EPR spectroscopy. *Biochemistry 51*, 138−148.
(62) Styring, S., Sjöholm, J., and Mamedov, F. (2012) Two tyrosines that changed the world: Interfacing the oxidizing power of photochemistry to water splitting in photosystem II. *Biochim. Biophys. Acta 1817*, 76−87.
(63) Groot, M. L., Pawlowicz, N. P., van Wilderen, L., Breton, J., van Stokkum, I. H. M., and van Grondelle, R. (2005) Initial electron donor and acceptor in isolated photosystem II reaction centers identified with femtosecond mid-IR spectroscopy. *Proc. Natl. Acad. Sci. U.S.A. 102*, 13087−13092.
(64) Holzwarth, A. R., Muller, M. G., Reus, M., Nowaczyk, M., Sander, J., and Rogner, M. (2006) Kinetics and mechanism of electron transfer in intact photosystem II and in the isolated reaction center: Pheophytin is the primary electron acceptor. *Proc. Natl. Acad. Sci. U.S.A. 103*, 6895−6900.
(65) Zech, S. G., Kurreck, J., Eckert, H. J., Renger, G., Lubitz, W., and Bittl, R. (1997) Pulsed EPR measurement of the distance between P_{680}^{+} and Q_A^{-} in photosystem II. *FEBS Lett. 414*, 454−456.
(66) Romero, E., Diner, B. A., Nixon, P. J., Coleman, W. J., Dekker, J. P., and van Grondelle, R. (2012) Mixed exciton-charge-transfer states in photosystem II: Stark spectroscopy on site-directed mutants. *Biophys. J. 103*, 185−194.
(67) Jeevarajan, A. S., Khaled, M., and Kispert, L. D. (1994) Simultaneous electrochemical and electron paramagnetic resonance studies of keto and hydroxy carotenoids. *Chem. Phys. Lett. 225*, 340−345.
(68) Shelaev, I. V., Gostev, F. E., Vishnev, M. I., Shkuropatov, A. Y., Ptushenko, V. V., Mamedov, M. D., Sarkisov, O. M., Nadtochenko, V. A., Semenov, A. Y., and Shuvalov, V. A. (2011) P_{680} (P(D1)P(D2)) and Chl(D1) as alternative electron donors in Photosystem II core complexes and isolated reaction centers. *J. Photochem. Photobiol., B 104*, 44−50.
(69) Raszewski, G., Diner, B. A., Schlodder, E., and Renger, T. (2008) Spectroscopic properties of reaction center pigments in photosystem II core complexes: Revision of the multimer model. *Biophys. J. 95*, 105−119.
(70) Nugent, J. H. A., Telfer, A., Demetriou, C., and Barber, J. (1989) Electron transfer in the isolated photosystem II reaction center complex. *FEBS Lett. 255*, 53−58.
(71) Brown, J. S., and Schoch, S. (1981) Spectral analysis of chlorophyll-protein complexes from higher plant chloroplasts. *Biochim. Biophys. Acta 636*, 201−209.
(72) van Dorssen, R. J., Plijter, J. J., Dekker, J. P., den Ouden, A., Amesz, J., and van Gorkom, H. J. (1987) Spectroscopic properties of chloroplast grana membranes and of the core of Photosystem II. *Biochim. Biophys. Acta 890*, 134−143.
(73) Kwa, S. L. S., Groeneveld, F. G., Dekker, J. P., van Grondelle, R., van Amerongen, H., Lin, S., and Struve, W. S. (1992) Steady-state and time-resolved polarized-light spectroscopy of the green plant light-harvesting complex II. *Biochim. Biophys. Acta 1101*, 143−146.
(74) Novoderezhkin, V. I., Dekker, J. P., and van Grondelle, R. (2007) Mixing of exciton and charge-transfer states in Photosystem II reaction centers: Modeling of Stark spectra with modified redfield theory. *Biophys. J. 93*, 1293−1311.
(75) Croce, R., Chojnicka, A., Morosinotto, T., Ihalainen, J. A., van Mourik, F., Dekker, J. P., Bassi, R., and van Grondelle, R. (2007) The low-energy forms of photosystem I light-harvesting complexes: Spectroscopic properties and pigment-pigment interaction characteristics. *Biophys. J. 93*, 2418−2428.
(76) Wientjes, E., Roest, G., and Croce, R. (2012) From red to blue to far-red in Lhca4: How does the protein modulate the spectral properties of the pigments? *Biochim. Biophys. Acta 1817*, 711−717.
(77) Romero, E., Mozzo, M., van Stokkum, I. H. M., Dekker, J. P., van Grondelle, R., and Croce, R. (2009) The origin of the low-energy form of photosystem I light-harvesting complex lhca4: Mixing of the lowest exciton with a charge-transfer state. *Biophys. J. 96*, L35−L37.

(78) McCauley, S. W., and Melis, A. (1987) Photosystem stoichiometry in higher plant chloroplasts. In *Progress in Photosynthesis Research* (Biggins, J., Ed.) Vol. *II*, pp 245−246, Martinus Nijhoff Publishers, Leiden, The Netherlands.